Technical Report No. 32-715

Comparisons of Experimental and Theoretical Aerodynamic Heating Results in Air-Carbon Dioxide Mixtures

E. A. Laumann

JET PROPULSION LABORATORY
CALIFORNIA INSTITUTE OF TECHNOLOGY
PASADENA, CALIFORNIA

January 15, 1965

Prepared Under Contract No. NAS 7-100
National Aeronautics & Space Administration

Technical Report No. 32-715

Comparisons of Experimental and Theoretical Aerodynamic Heating Results in Air-Carbon Dioxide Mixtures

E. A. Laumann

Bain Dayman, Jr.

Bain Dayman, Jr., Chief
Aerodynamic Facilities

JET PROPULSION LABORATORY
CALIFORNIA INSTITUTE OF TECHNOLOGY
PASADENA, CALIFORNIA

January 15, 1965

CONTENTS

I. Introduction 1

II. Experimental Data 4

III. Theoretical Calculations 4

IV. Comparison of Results 7

V. Conclusions 9

Nomenclature 9

References 11

FIGURES

1. Models used in the experiment: (a) Model I; (b) Model II; (c) Model III 2
2. Typical model installation 3
3. Specific heat vs % CO_2 5
4. Viscosity vs % CO_2 5
5. Thermal conductivity vs % CO_2 6
6. Prandtl number vs % CO_2 6
7. Enthalpy difference vs % CO_2 6
8. Mach number vs % CO_2 6
9. γ vs % CO_2 6
10. Stagnation point heat transfer vs % CO_2 7
11. Heat transfer distributions for Models I and III at $\alpha = 0$ deg 8
12. Heat transfer distributions for Model II at $\alpha = 0$ deg 8
13. Heat transfer distributions for Model III at $\alpha = 180$ deg 8

ABSTRACT

Convective heat transfer experiments were conducted in the Jet Propulsion Laboratory hypersonic wind tunnel in air–carbon dioxide mixtures. The mixtures were in chemical equilibrium, and the amounts of carbon dioxide in air were varied from 0% to 72% by volume. The convective heating of three different model shapes was measured, using calorimetric techniques.

The results of these experiments are compared with the stagnation point heating theory of Fay and Riddell, using the Lennard–Jones potential theory to evaluate the transport properties of the gas mixtures. The heat transfer distributions are compared to the theory of Lees.

I. INTRODUCTION

The design of planetary entry capsules is highly dependent upon the type and severity of the aerodynamic induced heat to which the capsule will be subjected during its high-velocity entry. Considerable effort is being expended to investigate that portion of the trajectory where both radiative and convective heating are present, and both theoretical and experimental information are becoming available concerning stagnation point aerodynamic heating at superorbital velocities.

The purpose of this Report is to describe the results of an investigation to determine the validity of making convective aerodynamic heating estimates for air–carbon dioxide gas mixtures using the theories developed and verified in air. The experimental convective heat transfer data described here were obtained at a nominal Mach number of 6 in air, with carbon dioxide added (up to 72% by volume). The stagnation enthalpy was approximately 7.8×10^6 ft^2/sec^2, and the unit free-stream Reynolds number was approximately 0.15×10^6/in. for all tests. Because the enthalpy levels were relatively low, the flow was in chemical equilibrium at all times. The theories that are compared with experimental results are the stagnation point theory of Fay and Riddell and the heat transfer distribution theory of Lees.

The experimental portion of this work was conducted in the Jet Propulsion Laboratory 21-in. hypersonic wind tunnel. This facility is a flexible-nozzle, continuous-flow facility capable of operating at Mach numbers from 4 to 11. Stagnation pressures of 650 psi and stagnation temperatures of 1300°F are possible. A detailed description of the tunnel is given in Ref. 1.

The experimental test data were obtained using the so-called transient heat transfer technique. This technique consisted of measuring the time rate of temperature change of a thin-skin metallic model. Prior to each test run, the model was cooled to a temperature below the recovery temperature. Details of the test technique are contained in Ref. 2.

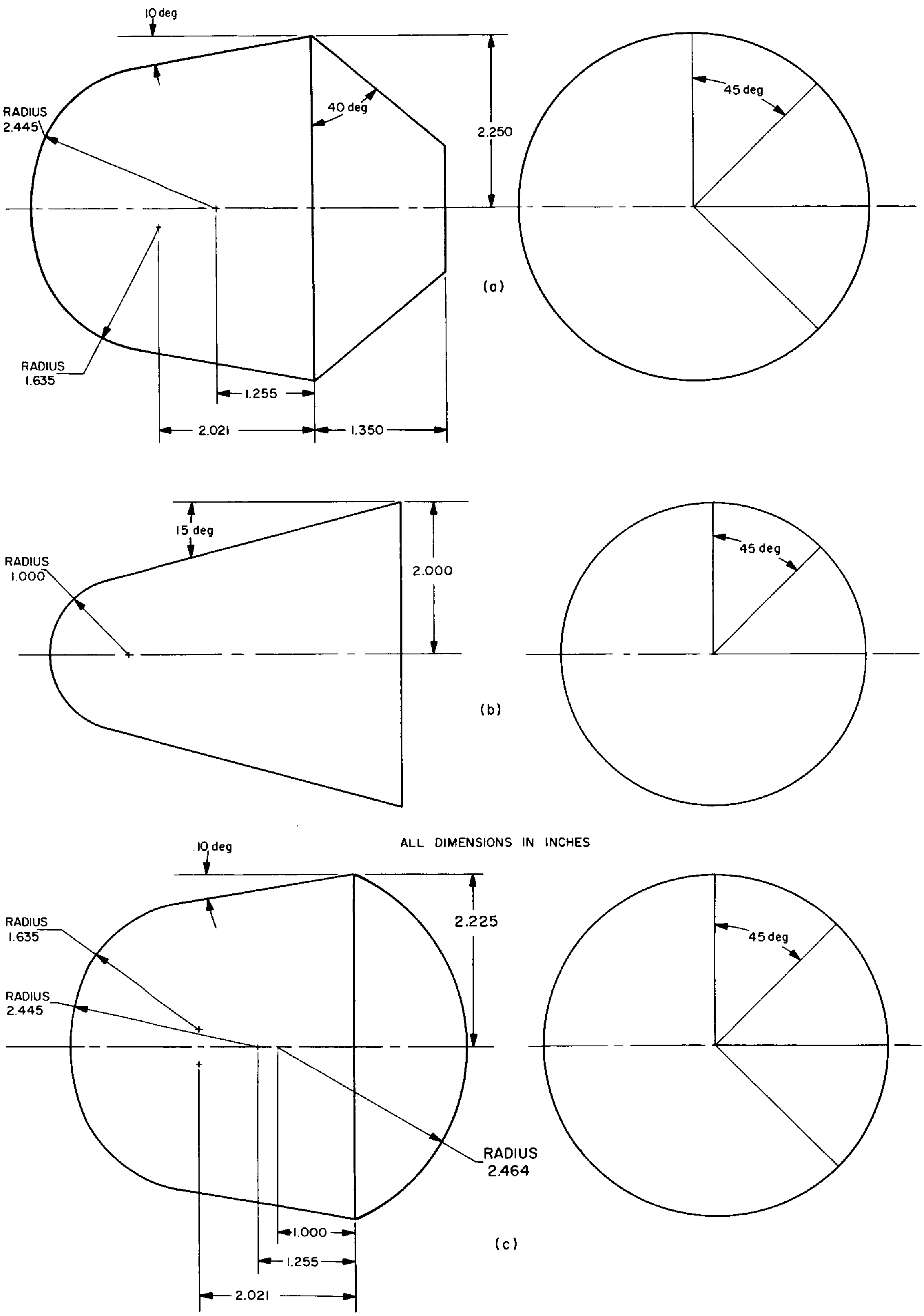

Fig. 1. Models used in the experiment: (a) Model I; (b) Model II; (c) Model III

The procedures followed for introducing significant amounts of carbon dioxide into the wind tunnel circuit, and the effects produced by doing so, are described in Ref. 3. Briefly, the procedure is to introduce liquid CO_2 downstream of the test section and to allow gaseous mixing to occur through the compression stages of the tunnel circuit. The nozzle shape is not adjusted to compensate for the changing γ.[1] This causes a reduction in the test rhombus Mach number, but flow calibrations show that the Mach number variation through the test rhombus remains very small.

Three model shapes (Fig. 1) were used for the experimental work. The models were constructed of electrolytic nickel with a uniform wall thickness of approximately 0.025 in. Local model wall temperatures were measured using 0.010-in. dia chromel–constantan thermocouples spot welded to the inner surface of the model wall. The thermocouples were located on several meridians of the axisymmetric models. The models were mounted in the wind tunnel on a vertical strut as shown in Fig. 2. This arrangement permitted angular rotation of any model from 0 deg to 180 deg.

[1]See Nomenclature for definitions of terms.

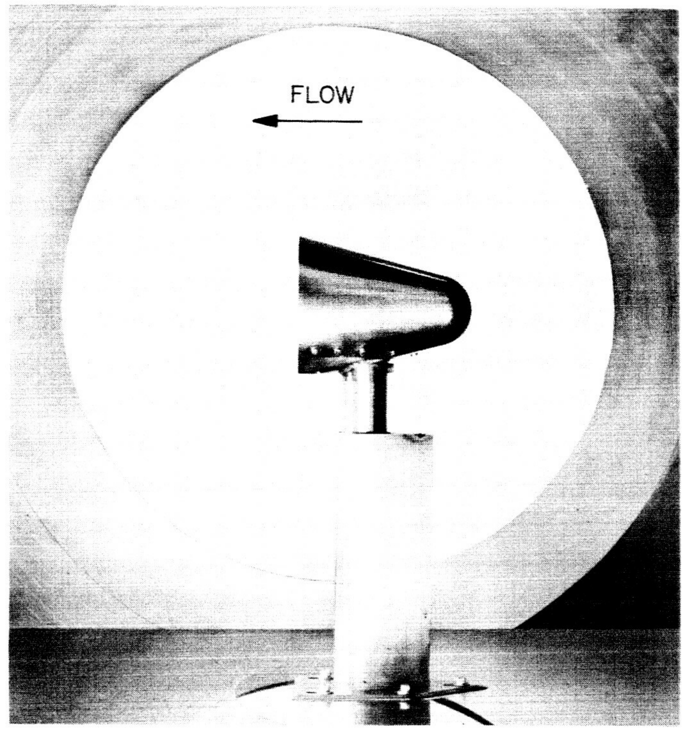

Fig. 2. Typical model installation

II. EXPERIMENTAL DATA

The thermocouple data, recorded every 0.05 sec during each run, were reduced and used to determine the rate of change of model surface temperature with time and subsequently to determine the calorimetric heat rates. Details of this procedure are described in Ref. 2. Model temperatures ranged between 500°R and 600°R for the data presented here.

Heat transfer data were obtained for each of the models at various angles of attack from 0 deg through 180 deg. Because the model support created a flow disturbance that was atypical of a model in free flight, all model temperatures measured at locations that lay in the vicinity of or behind the support bow shock were considered invalid. The same reasoning was used to invalidate all heating measurements in separated flow regions lying behind the support strut, because of the possibility of subsonic pressure disturbances.

The experimental data for Models I and II, obtained when the flat base was facing the oncoming stream, exhibited excessive scatter and are invalid. The flat base was not sufficiently strong to prevent physical deflection (oil canning) of the surface; the concave deflection was noticeable but not measurable. The experimental results showed enough scatter to indicate that unsteady flow existed over the concave surface under these conditions.

The worst-case inaccuracy of the experimental results is estimated to be ±6%, based upon the following factors:

uncertainties of material thermal properties	1.0%
uncertainty of model wall thickness	2.5%
uncertainty of temperature change rate	1.5%
conduction losses caused by non-zero model wall temperature gradients	1.0%

Other uncertainties are considered negligible compared to these.

III. THEORETICAL CALCULATIONS

The stagnation point convective heat transfer theory of Fay and Riddell (Ref. 4) was used as the basis of evaluation of the stagnation point heat transfer data presented in this Report. Because of the low test enthalpy, no dissociation was considered. The expression of stagnation point heat transfer was written as

$$h_s (R_s)^{1/2} = \frac{\dot{q}_s (R_s)^{1/2}}{T_s - T_w} = 0.76\,(Pr_w)^{-0.6} \times \frac{H_s - H_w}{T_s - T_w} (\rho_s \mu_s)^{0.4} (\rho_w \mu_w)^{0.1} \left[2\,\frac{(P_s - P)}{\rho_s} \right]^{0.25}$$

by assuming that a Bernoulli–Newtonian velocity gradient exists at the stagnation point.

The theoretical variation of heat transfer with CO_2 content was determined by calculating the thermal and transport properties of several air–CO_2 mixtures and by introducing these calculations into the above equation. The thermal properties were based on molecular ratios, and the transport properties were obtained using the Lennard–Jones potential theory as outlined in Ref. 5. In making the calculations, a binary mixture of air and CO_2 was assumed, rather than a multicomponent mixture of the several molecular elements involved. Reference 6 was used as a source for the properties of pure gases. For simplicity, the wall temperature was assumed to be 540°R for all wall-property calculations.

The specific heat, enthalpy, and Prandtl number were calculated as follows:

$$C_p = \left[\sum_i x_i \,(C_p/R)_i \right] [\Sigma\, x_i R_i]$$

$$H_s - H_w = \int_{T=540}^{1260} C_p \, dT$$

$$Pr_w = \frac{\mu_w C_{p_w}}{k_w}$$

The enthalpy difference integration was carried out by assuming a linear variation of C_p over intervals of 180°R. The results of all of the above calculations are shown in Fig. 3 through 7.

The wind tunnel nozzle flow was assumed to be best represented by the isentropic expansion of a perfect gas. The values of specific heat at constant pressure were obtained from Ref. 6 by assuming a reference pressure and temperature of 0.4 atm and 360°R respectively, and the ratios of specific heats for the various air–CO_2 mixtures were calculated as

$$\gamma = \frac{C_p/R}{C_p/R - 1}$$

The Mach number, static pressure, stagnation point density, and wall stagnation point density were determined from measured values of total pressure, pitot pressure, and total temperature. The calculated variations of Mach number and γ in the test section are shown in Fig. 8

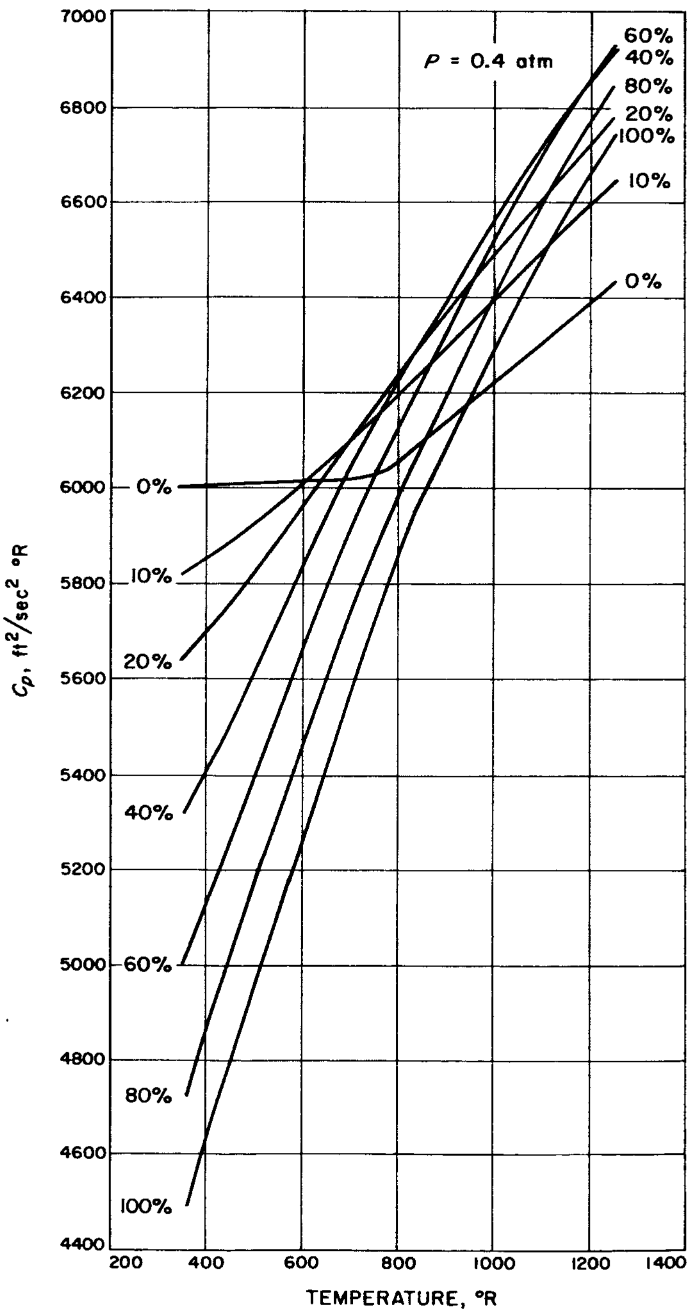

Fig. 3. Specific heat vs % CO_2

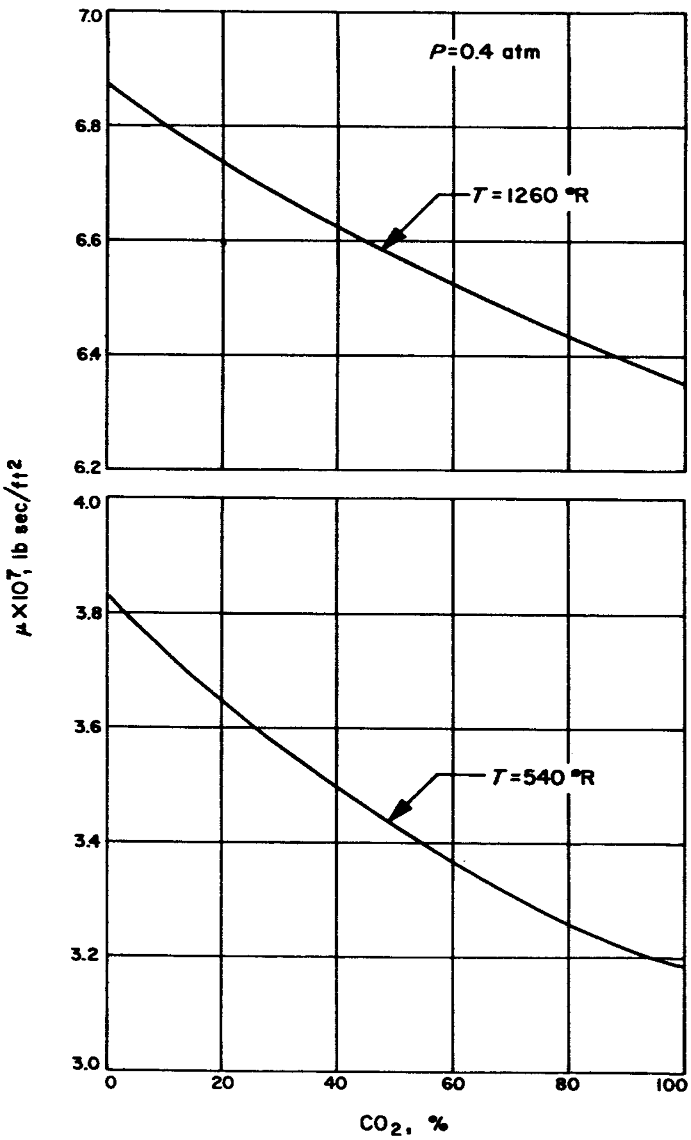

Fig. 4. Viscosity vs % CO_2

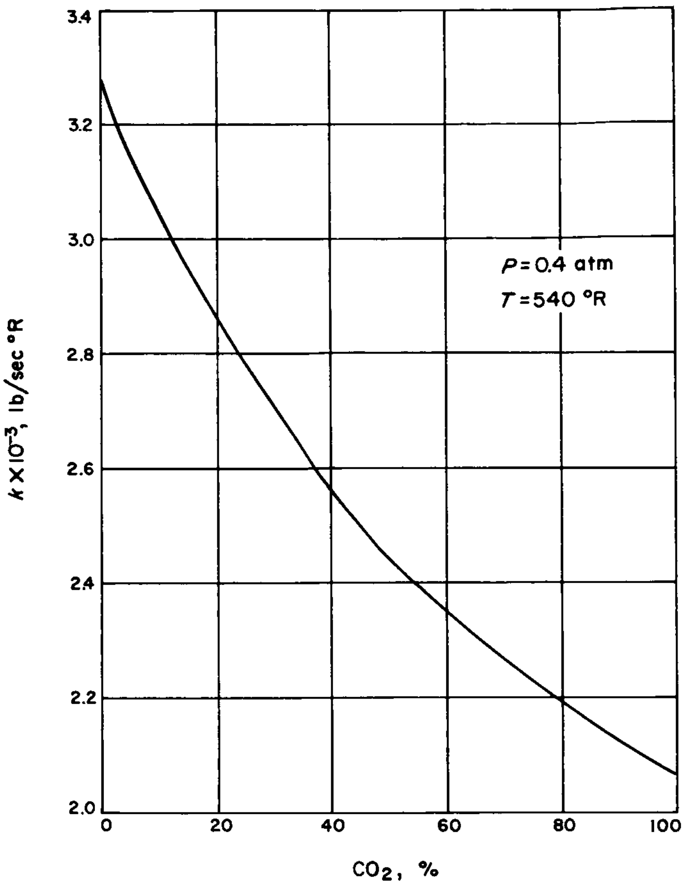

Fig. 5. Thermal conductivity vs % CO_2

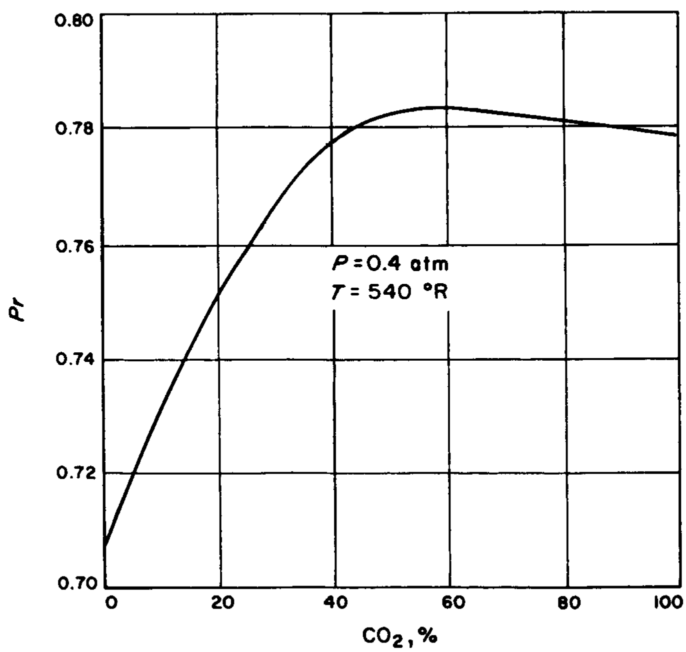

Fig. 6. Prandtl number vs % CO_2

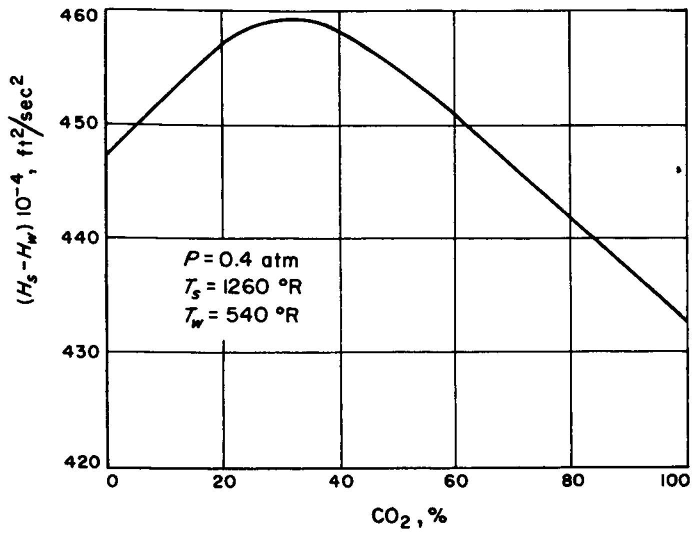

Fig. 7. Enthalpy difference vs % CO_2

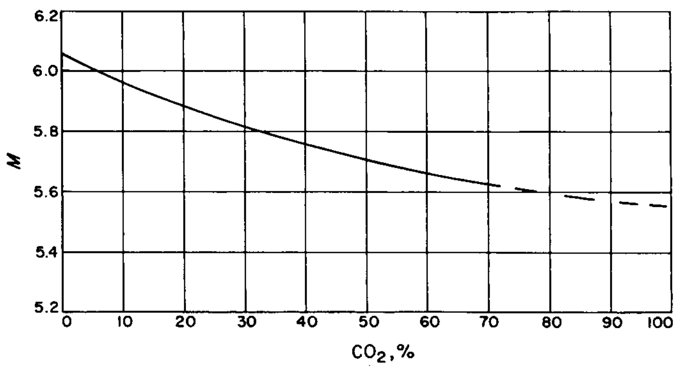

Fig. 8. Mach number vs % CO_2

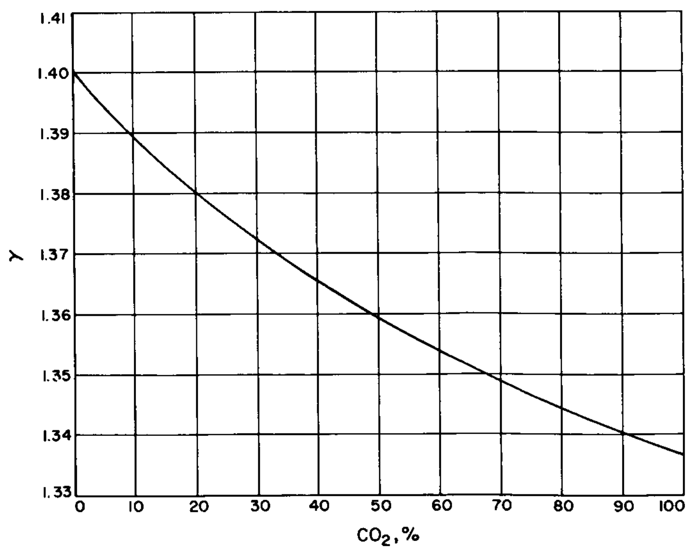

Fig. 9. γ vs % CO_2

and 9. All experimental data were obtained under the following constant tunnel conditions:

stagnation pressure	174 psi
pitot pressure	5.01 psi
stagnation temperature	1260°R

The heat transfer distribution calculations were based upon the theory of Lees (Ref. 7), assuming a modified Newtonian pressure distribution. The heat transfer distribution was written as

$$h_l = \frac{\left(\frac{P}{P_{e_l}}\right)\theta_l y}{2\int_{\theta=0}^{\theta_l}\left(\frac{P_e}{P_s}\right)\theta y^2\, d\theta}\,[h_s (R_s)^{1/2}]$$

The integration was carried out numerically, with the actual body coordinates of the conical sections adjusted to conform to the virtual apex geometry.

IV. COMPARISON OF RESULTS

The experimental convective heat transfer results are presented in Fig. 10. Superimposed on these results are the theoretical curves calculated for the noted test conditions. The experimental data for Model II at 0 deg and for Model III at 180 deg show excellent agreement with theory. The data for Models I and III at 0 deg show only good agreement with theory; this is due to the inaccuracy in Bernoulli–Newtonian velocity gradients for very blunt noses, as was pointed out in Ref. 8, where the gradient becomes no longer inversely proportional to the square root of the nose radius. By assuming a Newtonian sonic line position, a Boison and Curtiss effective nose radius can be determined for Models I and III. Substituting this dimension for the geometric stagnation point radius in the Fay and Riddell theory, the dashed curve in Fig. 10 is obtained. Thus the experiment shows excellent agreement with theory when the stagnation point velocity gradient is more accurately determined.

The windward heat transfer distributions obtained for Models I and III (geometrically similar) at 0 deg are presented in Fig. 11, together with the calculated theoretical distributions. Excellent agreement exists between experiment and theory, with two notable exceptions. The theory consistently overestimates heating in the region of l/D values of 0.25 to 0.40 and underestimates heating in the region of the torus–cone intersection ($l/D = 0.55$). Other data (not presented), obtained with intermediate amounts of CO_2, fall within the scatter band of the data presented here. The presence of CO_2 in the gas flow has a negligible effect on the aerodynamic heating distribution.

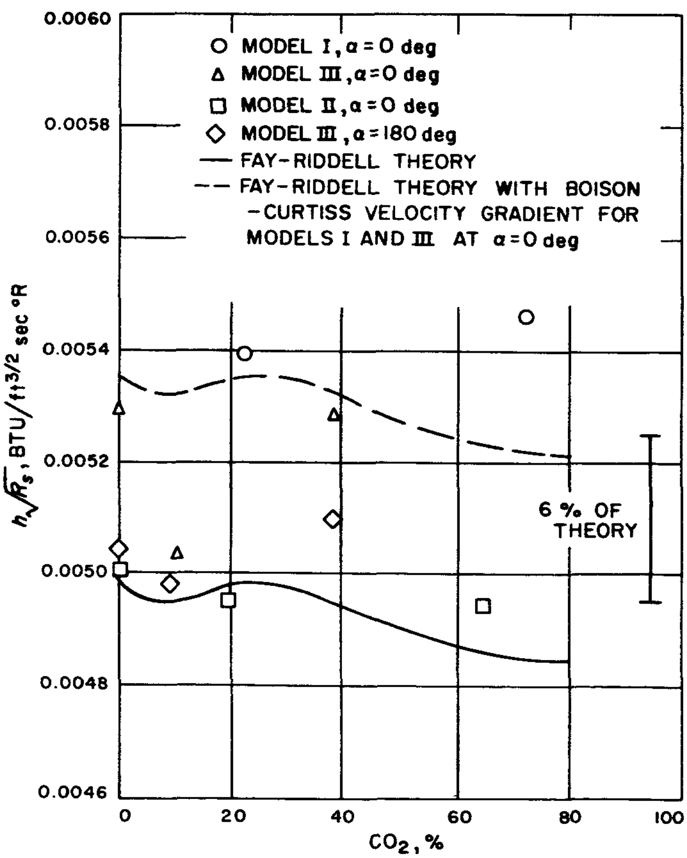

Fig. 10. Stagnation point heat transfer vs % CO_2

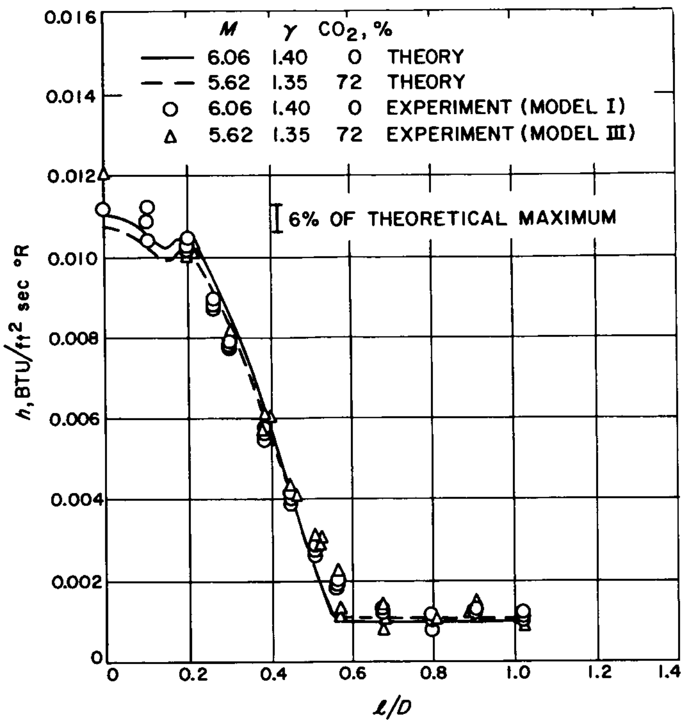

Fig. 11. Heat transfer distributions for Models I and III at $\alpha = 0$ deg

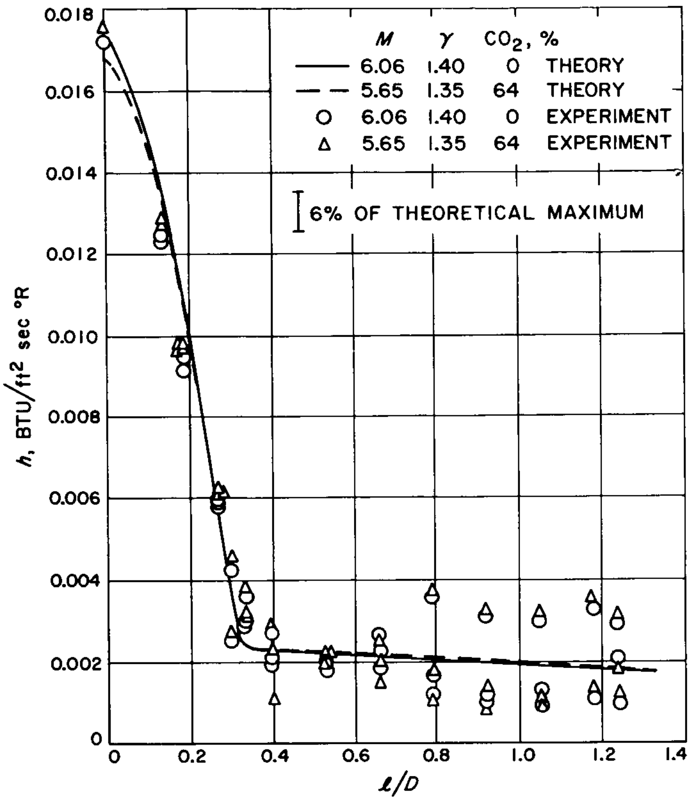

Fig. 12. Heat transfer distributions for Model II at $\alpha = 0$ deg

The windward heat transfer distributions obtained for Model II, together with the theoretical distributions, are presented in Fig. 12. Again, agreement between experiment and theory is very good. The theory, however, consistently overestimates heating in the region of l/D values of 0.1 to 0.2 and underestimates heating in the region of the hemisphere–cone intersection. The rather wide variations in experimental heating data between l/D values of 0.6 and 1.3 are of unknown origin, but they can probably be attributed to warping of the model shape due to an improper fit between the model and the support fitting. All of the data that show higher heating rates in this region lie along the meridian closest to the model support. The addition of CO_2 to the gas flow produces a negligible effect on the heating at all measuring stations, not only for the data presented here but also for several other intermediate values of CO_2 content under which heating data were measured.

Figure 13 presents the experimental data and the theoretical calculations for Model III at 180 deg. Again the experimental results verify the theory extremely well. The theory slightly overestimates heating at l/D values of 0.4 to 0.6.

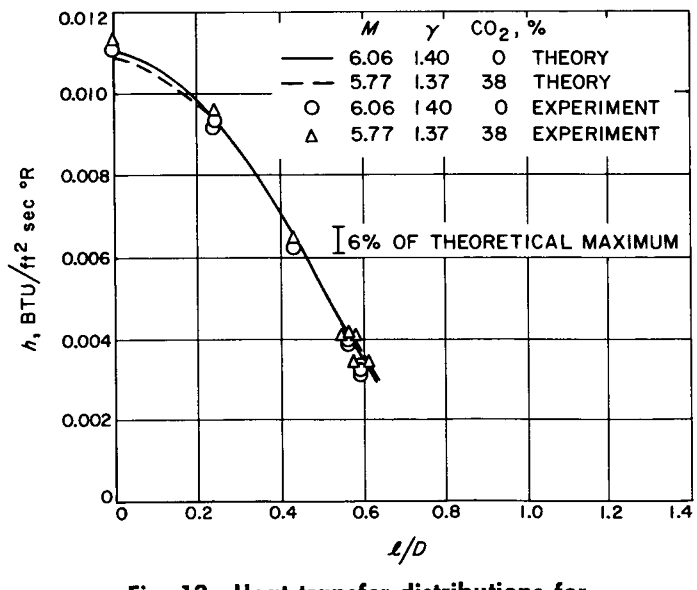

Fig. 13. Heat transfer distributions for Model III at $\alpha = 180$ deg

Additional experimental data were obtained at angles of attack in increments of 20 deg between 0 deg and 180 deg. All of these data show a negligible effect on heating when any amount of CO_2 is added to the flowing gas.

V. CONCLUSIONS

The convective heat transfer to blunt entry bodies can be predicted for any air–CO_2 mixture with an accuracy of approximately 5%, using the theories of Fay and Riddell and Lees at moderate enthalpy levels. The Lennard–Jones potential theory adequately predicts the transport properties of the mixtures at these enthalpy levels.

The total variation of stagnation point heat transfer and the heat transfer distribution are shown to be negligibly affected by the presence of large amounts of CO_2. The CO_2-induced Mach number effect is also very small and is reflected primarily in the minor variations of the Newtonian pressure gradient.

The data presented by Collins and Horton (Ref. 9) also show that the addition of CO_2 to the flowing fluid has a negligible effect on convective heat transfer at the stagnation point. These data were obtained in a shock tube under stagnation enthalpy conditions 25 to 50 times greater (or flight velocities 5 to 7 times greater) than those of the tests reported here.

It must be concluded, therefore, that the presence of unknown amounts of carbon dioxide in a planetary atmosphere need not be of concern to a planetary capsule heat-shield designer for entry velocities below 30,000 ft/sec.

NOMENCLATURE

- C_p specific heat (ft²/sec² °R)
- D major diameter of model (ft)
- H enthalpy (ft²/sec²)
- h heat transfer coefficient (BTU/ft²sec °R)
- i indicates a specific gas
- k thermal conductivity (lb/sec °R)
- l surface distance from stagnation point (ft)
- M Mach number
- P pressure (lb/ft²)
- Pr Prandtl number
- $\dot{q}$ heat transfer rate (BTU/ft² sec)
- R gas constant (ft²/sec² °R)
- s conditions immediately behind the normal shock
- T temperature (°R)
- w conditions at the model wall
- x mass fraction of a gas
- y radial distance from model axis of symmetry to model surface, measured normal to axis of symmetry (ft)
- α angle of attack of axis of symmetry
- γ ratio of specific heats
- ρ density (lb sec²/ft⁴)
- μ viscosity (lb sec/ft²)
- θ angle between the body surface and the normal to the free-stream wind vector (rad)

REFERENCES

1. "Wind Tunnel Facilities at the Jet Propulsion Laboratory," *Technical Release No. 34-257,* Jet Propulsion Laboratory, Pasadena, California, April 18, 1961.
2. Laumann, E. A., "Determining Aerodynamic Heating Rates Using Calorimetric Models in the Jet Propulsion Laboratory Hypersonic Wind Tunnel," *Technical Memorandum No. 33-121,* Jet Propulsion Laboratory, Pasadena, California, March 7, 1963.
3. Hanks, D., Herrera, G., and Koester, H., "The Use of a Conventional Wind Tunnel as a Multigas Facility," *Technical Memorandum No. 33-145,* Jet Propulsion Laboratory, Pasadena, California, April 8, 1963.
4. Fay, J. A. and Riddell, F. R., "Theory of Stagnation Point Heat Transfer in Dissociated Air," *Journal of the Aerospace Sciences,* Vol. 25, No. 2, p. 73, February, 1958.
5. Hirschfelder, J. O., Curtiss, C. F., and Byrd, R. B., *Molecular Theory of Gases and Liquids,* John Wiley and Sons, Inc., New York, 1954.
6. Hilsenrath, J. et al., "Tables of Thermal Properties of Gases," Circular No. 564, U. S. Bureau of Standards, 1955.
7. Lees, L., "Laminar Heat Transfer Over Blunt Nosed Bodies at Hypersonic Flight Speeds," *Jet Propulsion,* Vol. 26, pp. 259–269, 1956.
8. Boison, J. C. and Curtiss, H. A., "An Experimental Investigation of Blunt Body Stagnation Point Velocity Gradient," *ARS Journal,* Vol 29, No. 1, pp. 130–135, February, 1959.
9. Collins, D. J. and Horton, T. E., "Experimental Convective Heat Transfer Measurements," *AIAA Journal,* Vol. 2, No. 11, pp. 2046–2047, November, 1964.